A Template for Stabilization of a Peptide α-Helix: Synthesis and Evaluation of Conformational Effects by Circular Dichroism and NMR

Richard E. Austin,[†] Rachael A. Maplestone,[†] Andrea M. Sefler,[†] Kim Liu,[†] Witold N. Hruzewicz,[†] Corey W. Liu,[‡] Ho S. Cho,[‡] David E. Wemmer,[‡] and Paul A. Bartlett*,[†]

Contribution from the Department of Chemistry, University of California, Berkeley, California 94720-1460, and Structural Biology Division, Lawrence Berkeley National Laboratory, 1 Cyclotron Road, Berkeley, California 94720-5230

Received December 9, 1996. Revised Manuscript Received April 21, 1997[⊗]

Abstract: The bicyclic diacid **1** was designed as a semi-rigid template for the hydrogen-bonding pattern of a peptide α-helix. The protected precursor **7** was synthesized in eight steps from *tert*-butyl 3,5-dimethoxybenzoate and linked to L-alanine and L-lactic acid to provide derivatives appropriate for coupling to a peptide. Both the amide **8-N** and the ester **12-O** were obtained in each of the four diastereomeric forms. The structure of **R,R-8-N** was determined by X-ray crystallography, which facilitated assignment of the diastereomers and confirmed the intended conformational effects of the quaternary methyl groups. The bicyclic amide and ester derivatives were appended to the peptide EALAKA-NH_2, and their influence on the conformation was evaluated in aqueous solution using circular dichroism and NMR. The amide analogs have only a slight effect on the appended peptide, whereas the ester-linked template in **S,S-9-O** induces 32−50% helical character at 23 °C and 49−77% at 0 °C, depending on the method of determination; significant helical character persists even at 70 °C. The ability of the template **1** to induce the helical conformation is related to its structural and electronic complementarity to the N-terminus of the peptide; templating ability disappears when the carboxylate in **S,S-9-O** is protonated, and it is not observed in the dimethylamide **S,S-9-N-a**. The structural and dynamical properties of conjugate **S,S-9-O** were studied by NMR and compared with those of the acetylated heptapeptide **13**. The dispersion and temperature dependence of amide hydrogen chemical shifts and the pattern observed for intra- and inter-residue nuclear Overhauser enhancements are all consistent with a significant population of helical conformers within the conformational ensemble of conjugate **S,S-9-O**, in contrast to the unstructured peptide **13**. The generalized order parameter S^2 was derived for each residue from the ^{15}N T_1 and T_2 relaxation rate constants and $^1H-^{15}N$ heteronuclear NOEs determined for the ^{15}N-labeled derivative of **S,S-9-O**; these parameters demonstrate a high degree of conformational rigidity along the peptide chain at 4 °C, with relative motion increasing for the C-terminal residues. These data are consistent with the chiroptical studies and demonstrate that the template is exceptionally effective in inducing helical behavior in an appended peptide.

The α-helix, a classic element of protein secondary structure, represents an unstable conformation of a small peptide in the general case;[1−3] without additional constraints, the modest advantage of internal hydrogen bonding and side chain−side chain interactions in the helix is insufficient to overcome the penalty of conformational restriction.[4−6] In peptides that do show significant helical character, this instability is manifested at the end of the helix where considerable "fraying" of the terminal residues occurs.[7,8] Just as a shoelace is stabilized against unraveling by the aglet, so can an α-helix be stabilized by side chain−side chain cross-links[9−13] or by other structural elements that reduce the conformational freedom of the terminal hydrogen-bonding groups.[14] Synthetic templating moieties have been reported by Kemp[15−17] and by Müller[18] and their co-workers, and "capping boxes" comprised of normal amino acid sequences have been elucidated as well.[19,20]

In this paper, we describe the synthesis and evaluation of the hexahydroindol-4-one 3,6-diacid **1** and some of its derivatives as helix templates, to be appended to the N-terminus of a peptide chain (Figure 1b). The carboxylate at C-6, vinylogous

[⊗] Abstract published in *Advance ACS Abstracts,* June 15, 1997.

(1) Naider, F.; Goodman, M. In *Bioorganic Chemistry*; Van Tamelen, E. E., Ed., Academic Press: New York, 1977; Vol III, p 177.
(2) Goodman, M.; Schmitt, E. E.; Yphantis, D. A. *J. Am. Chem. Soc.* **1962**, *84*, 1962.
(3) Zimm, B. H.; Bragg, J. K. *J. Chem. Phys.* **1959**, *31*, 526−535.
(4) Yang, A.-S.; Honig, B. *J. Mol. Biol.* **1995**, *252*, 351−365.
(5) Scholtz, J. M.; Baldwin, R. L. *Annu. Rev. Biophys. Biomol. Struct.* **1992**, *21*, 95−118.
(6) Creamer, T. P.; Rose, G. D. *Proc. Nat. Acad. Sci. U.S.A.* **1992**, *89*, 5937−5941.
(7) Waltho, J. P.; Feher, V. A.; Merutka, G.; Dyson, H. J.; Wright, P. E. *Biochemistry* **1993**, *32*, 6337−6347.
(8) Young, W. S.; Brooks, C. L., III *J. Mol. Biol.* **1996**, *259*, 560−572.
(9) Ruan, F.; Chen, Y.; Hopkins, P. B. *J. Am. Chem. Soc.* **1990**, *112*, 9403−9404.
(10) Ghadiri, M. R.; Fernholz, A. K. *J. Am. Chem. Soc.* **1990**, *112*, 9633−9635.
(11) Jackson, D. Y.; King, D. S.; Chmielewski, J.; Singh, S.; Schultz, P. G. *J. Am. Chem. Soc.* **1991**, *113*, 9391−9392.
(12) Chorev, M.; Roubini, E.; McKee, R. L.; Gibbons, M. E.; Caulfield, M. P.; Rosenblatt, M. *Biochemistry* **1991**, *30*, 5968−5974.
(13) Bracken, C.; Gulyás, J.; Taylor, J. W.; Baum, J. *J. Am. Chem. Soc.* **1994**, *116*, 6431−6432.
(14) Schneider, J. P.; Kelly, J. W. *Chem. Rev.* **1995**, *95*, 2169−2187.
(15) Kemp, D. S.; Curran, T. P.; Davis, W. M.; Boyd, J. G.; Muendel, C. *J. Org. Chem.* **1991**, *56*, 6672−6682.
(16) Kemp, D. S.; Curran, T. P.; Boyd, J. G.; Allen, T. J. *J. Org. Chem.* **1991**, *56*, 6683−6697.
(17) Kemp, D. S.; Allen, T. J.; Oslick, S. L. *J. Am. Chem. Soc.* **1995**, *117*, 6641−6657.
(18) Müller, K.; Obrecht, D.; Knierzinger, A.; Stankovic, C.; Spiegler, C.; Bannwarth, W.; Trzeciak, A.; Englert, G.; Labhardt, A. M.; Schoenholzer, P. *Perspect. Med. Chem.* **1993**, 513−31.
(19) Zhou, H. X.; Lyu, P.; Wemmer, D. E.; Kallenbach, N. R. *Proteins* **1994**, *18*, 1−7.
(20) Harper, E.; Rose, G. D. *Biochemistry* **1993**, *32*, 7605−7609.

S0002-7863(96)04231-X CCC: $14.00

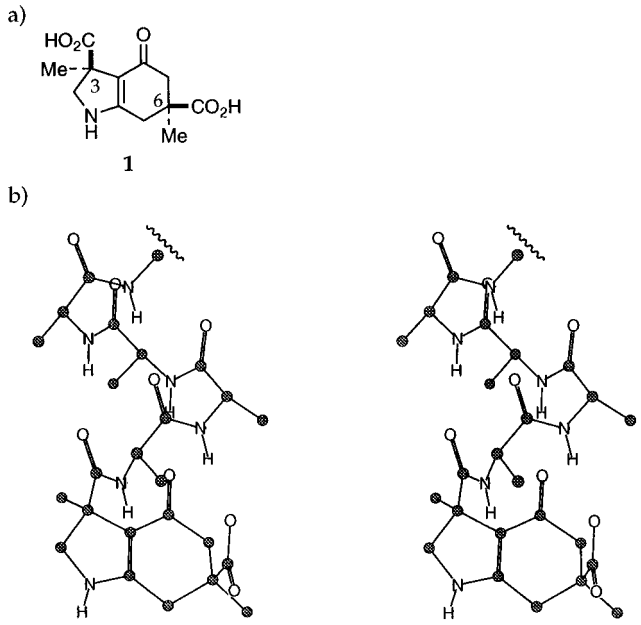

Figure 1. The helix "aglet": (a) structure of parent compound **1** (*S,S*-isomer); (b) model of α-helical conformation of peptide conjugate.

Scheme 1

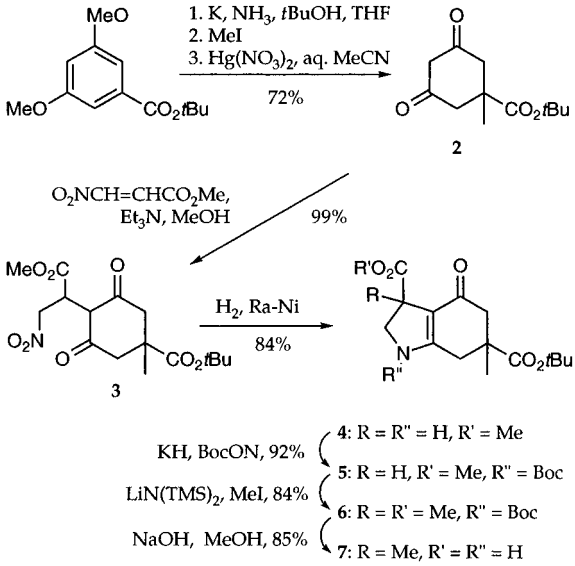

amide, and carbonyl group at C-3 were designed to mimic three successive peptide carbonyls in the α-helical conformation, and the negative charge was expected to complement the positive helix dipole.[21−25] The methyl substituents were placed at C-6 and C-3 to favor the pseudoaxial disposition of the carboxylate moiety and to disfavor the undesired torsional conformer at the C-3 carbonyl position.

Synthesis

The synthesis of a protected form of **1** is depicted in Scheme 1. Birch-type reductive alkylation of *tert*-butyl 3,5-dimethoxybenzoate was followed by hydrolysis of the enol ethers to give the functionalized cyclohexane-1,3-dione **2** in 34% overall yield.

Scheme 2

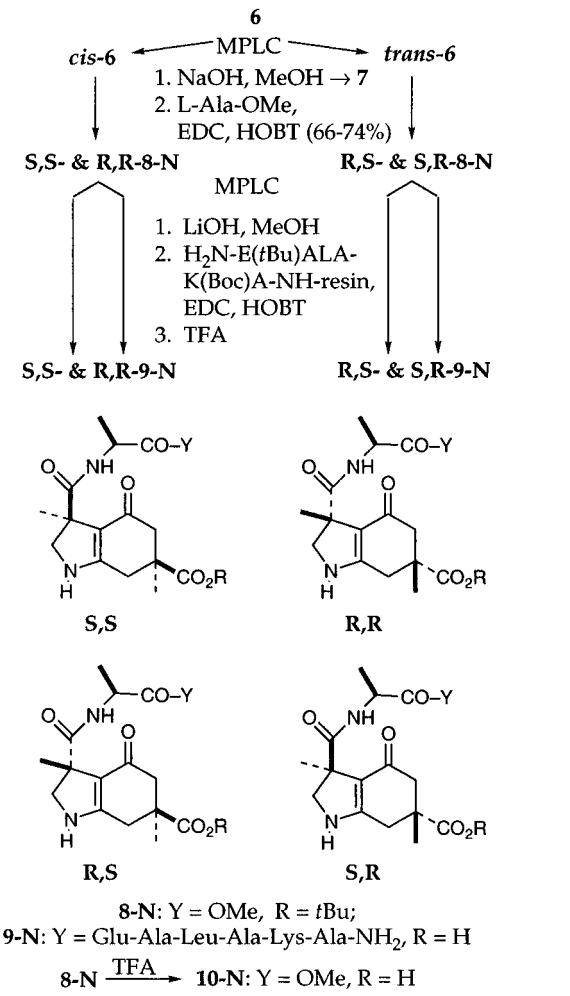

This active methylene compound was added to methyl β-nitroacrylate,[26] with the nitro group as the Michael acceptor, to give adduct **3**. Catalytic reduction of the nitro group was followed by spontaneous cyclization to the hexahydroindolone **4**. After protection of the nitrogen (→ **5**), the quaternary methyl was introduced by enolate alkylation to give **6**.[27] Alkaline hydrolysis of **6** removed the Boc group from the vinylogous amide as well as the methyl ester, affording the monoacid **7** which was coupled to L-alanine methyl ester with carbodiimide activation.

No stereochemical control was exerted during the racemic synthesis of the bicyclic template, but the *cis* and *trans* isomers of diester **6** were separated by MPLC prior to coupling with L-alanine. The diastereomers of **8-N** (Scheme 2) were separated in turn so that all four stereoisomers were available in pure form. An X-ray structure of one of these isomers, which proved to be **R,R-8-N** (Figure 2), allowed us to assign this and the *S,S*-diastereomer. This structure also confirmed that the quaternary

(21) Wada, A. *Adv. Biophys.* **1976**, *9*, 1−63.
(22) Hol, W. G. J.; Van Duijnen, P. T.; Berendsen, H. J. C. *Nature (London)* **1978**, *273*, 443−446.
(23) Åqvist, J.; Kuecke, H.; Quiocho, F. A.; Warshel, A. *Proc. Natl. Acad. Sci. U.S.A.* **1991**, *88*, 2026−2030.
(24) Nicholson, H.; Anderson, D. E.; Dao-pin, S.; Matthews, B. W. *Biochemistry* **1991**, *30*, 9816−9828.
(25) Lockhart, D. J.; Kim, P. S. *Science* **1993**, *260*, 198−202.
(26) McMurry, J. E.; Musser, J. H. *Org. Synth.* **1977**, *56*, 65−68.
(27) Direct incorporation of this methyl group at the Michael addition step, by using methyl β-nitromethacrylate,[28] was thwarted by isomerization of this material under the basic reaction conditions to methyl α-(nitromethyl)acrylate, with ensuing addition-elimination to give **i**.

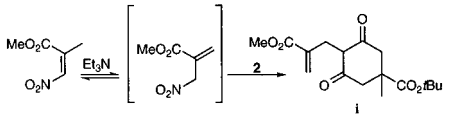

i

(28) Bonetti, G. A.; DeSavigny, C. B.; Michalski, C.; Rosenthal, R. *J. Org. Chem.* **1968**, *33*, 237−243.

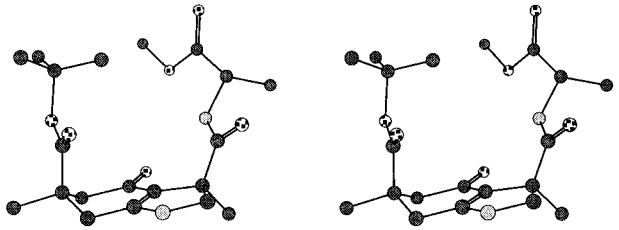

Figure 2. Solid state conformation of **R,R-6-N**.

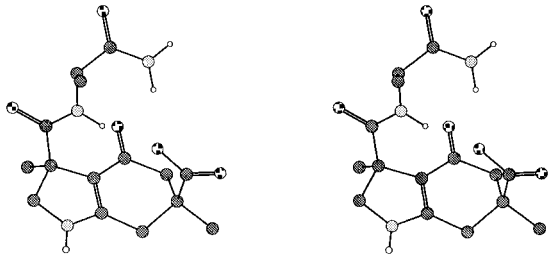

Figure 3. Potential 3_{10}-type hydrogen-bonding pattern for amide-linked conjugate **S,S-9-N**.

methyls induce the desired axial orientation of the carboxyl group at C-6. No structural information was obtained that allowed us to assign the *R,S*- and *S,R*-diastereomers directly.[29]

The sequence EALAKA-NH_2[30,31] was selected as the test sequence, since it incorporates residues that are predominantly helix-stabilizing (Ala and Glu-Lys salt bridge); the helix-neutral leucine was included to provide some differentiation for NMR analysis, and the charged residues to aid in solubilization as well. This peptide was synthesized on Rink-amide resin according to standard protocols, with *tert*-butyl ester and Boc protection on the glutamate and lysine residues, respectively, and then coupled with the diastereomeric alanine adducts **8-N**. Trifluoroacetic acid detached and deprotected the peptide conjugates **9-N**, which were purified by reverse phase HPLC.

Characterization by Circular Dichroism

The helical character of the template peptides **9-N** in aqueous solution was evaluated from their CD spectra, correcting for contributions from the templates themselves by subtracting the spectra of the alanine-coupled derivatives **10-N**. All four diastereomers show ca. 10−12% helical character at 23 °C; there is increased helicity at 0 °C, but still no significant difference between the stereoisomers. The template, in short, does not work in this context. Modeling studies with **S,S-8-N** suggested that an intratemplate hydrogen-bonded conformation (Figure 3) is readily accessible energetically; this conformation corresponds to the hydrogen-bonding pattern of a 3_{10} helix, rather than the desired α-pattern, and could be responsible for the ineffectiveness of the template in stabilizing the helix. The ester-linked derivatives **9-O** were therefore synthesized to circumvent this possibility.

Because of the lower nucleophilicity of the lactate hydroxyl group and the more vigorous conditions required for the coupling reaction, the vinylogous amide nitrogen of **7** had to be protected as the Boc derivative, **11**, prior to esterification (Scheme 3). The carboxyl group was activated with trichlorobenzoyl chloride and the coupling with methyl L-lactate was

(29) The tentative basis for assignment of *R,S*- and *S,R*-diastereomers was the *slightly* greater ellipticity observed when the former was conjugated to a longer peptide as {template}-AEAAAKEAAAKY-amide (data not shown).

(30) Marqusee, S.; Baldwin, R. L. *Proc. Natl. Acad. Sci. U.S.A.* **1987**, *84*, 8898−8902.

(31) Shoemaker, K. R.; Kim, P. S.; York, E. J.; Stewart, J. M.; Baldwin, R. L. *Nature* **1987**, *326*, 563−567.

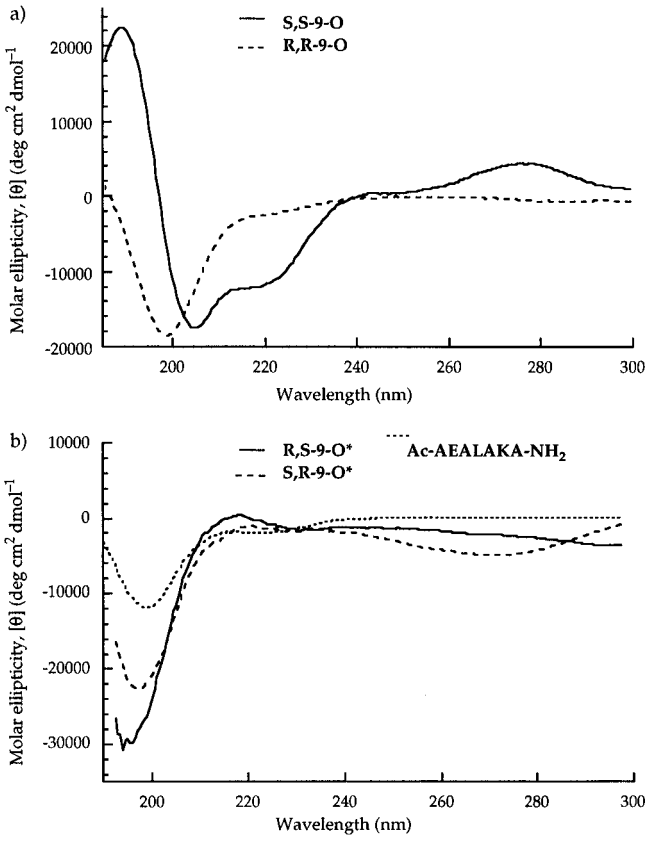

Figure 4. Circular dichroism spectra of templated peptides **9-O** at 0 °C (1 mM phosphate buffer, pH 5) corrected for the contributions of the corresponding diastereomers of **10-O**: (a) **S,S-9-O** (63 μM) and **R,R-9-O** (64 μM); (b) **R,S-9-O** (83 μM), **S,R-9-O** (94 μM), and acetylated heptapeptide (137 μM) (the asterisk denotes that the stereochemical assignments of *R,S*- and *S,R*-diastereomers are tentative).

Scheme 3

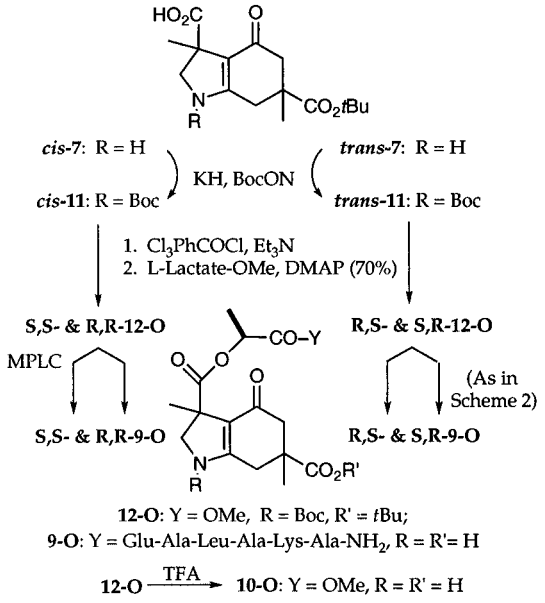

catalyzed by 4-(dimethylamino)pyridine (DMAP) to give **12-O**. These diastereomers were separated by MPLC and assigned by correlation with the amides **8-N** by alkaline hydrolysis to **7** and coupling to L-alanine methyl ester. The lactate methyl esters of **12-O** were carefully saponified, the templates were coupled to the hexapeptide, and the oxygen-linked conjugates **9-O** were isolated and purified as described above for the amides **9-N**.

Table 1. Molar Ellipticities at 222 nm and Percent Helicity for Template Peptides **9-N** and **9-O**

peptide	$[\Theta]_{222}$ (23 °C)[c]	helicity (%)[d]	$[\Theta]_{222}$ (0 °C)[c]	helicity (%)[d]
S,S-9-N[a]	−3290	13	−6200	25
R,R-9-N[a]	−2913	12	−3100	12
S,S-9-O[b]	−8109	32	−11143	49
R,R-9-O[b]	−1450	6	−2	0
Ac-AEAKALA-NH$_2$ (13)			−1966	8

[a] Measured in 0.1 M KCl, 50 mM potassium phosphate buffer, pH 5.2. [b] Measured in 1.05 mM potassium phosphate buffer, pH 5. [c] In (deg cm^2)/dmol, corrected for contribution from corresponding template-Ala or template-Lac derivative, **10-N** or **10-O**. [d] Calculated from ratio $[\Theta]_{222}/[\Theta]_{max}$, where $[\Theta]_{max} = -39\,500 \times [1 - (2.57/n)]$ (=25 000 for $n = 7$).[37,38,76]

Replacement of the amide NH with the ester oxygen has a dramatic effect on the helical character of the conjugates (Figure 4). In aqueous buffer at pH 5.2, the *S,S*-conjugate of **9-O** is 32% helical at 23 °C, increasing to 50% at 0 °C, according to the molar ellipticity at 222 nm (Table 1). Moreover, there are significant differences between the diastereomers, since the CD spectrum of the conjugate with the enantiomeric template, **R,R-9-O**, is that of a random coil. The *S,R*- and *R,S*-diastereomers also show no significant helical character, nor does the *N*-acetyl analog. The ellipticity measured for **S,S-9-O** at 222 nm is directly proportional to concentration over the range 8.6−272 μM, which suggests that the observed helicity does not result from aggregation. Moreover, such a large distinction between the diastereomers and the ester- and amide-linked analogs would not be expected if the helicity observed in **S,S-9-O** were due to aggregation.

The form of the CD curve for **S,S-9-O** below 250 nm is that expected for an α-helix and quite distinct from the 3_{10}-pattern recently described.[32] The helical conjugate **S,S-9-O** shows positive ellipticity from 270 to 290 nm. This band disappears when the helical character is lost (e.g., on titration; see Figure 6), and it is not observed for the diastereomeric conjugate **R,R-9-O**, even when a helix is induced in the latter by trifluoroethanol (see Figure 5b). The vinylogous amide of the bicyclic cap ($\lambda_{max} = 305$ nm) is presumably responsible for this band, which reflects the different asymmetric environment of the chromophore in the templated helix than in the control compund **10-O**.[33]

The degree of helical character observed for this conjugate is unprecedented for such a short peptide in aqueous solution: the seven residues (if lactate is counted) constitute less than two turns of an α-helix. Indeed, it is not clear if the equation for helicity is appropriate in the present case (Table 1), since it is parameterized from considerably longer peptides. An alternative estimation of the percent helicity can be obtained by comparison of the conjugates under conditions in which maximal helicity can be expected, e.g., in the presence of trifluoroethanol (TFE) (Figure 5).[34−36] Both the **S,S-9-O** and **R,R-9-O** conjugates show enhanced, and comparable, helical

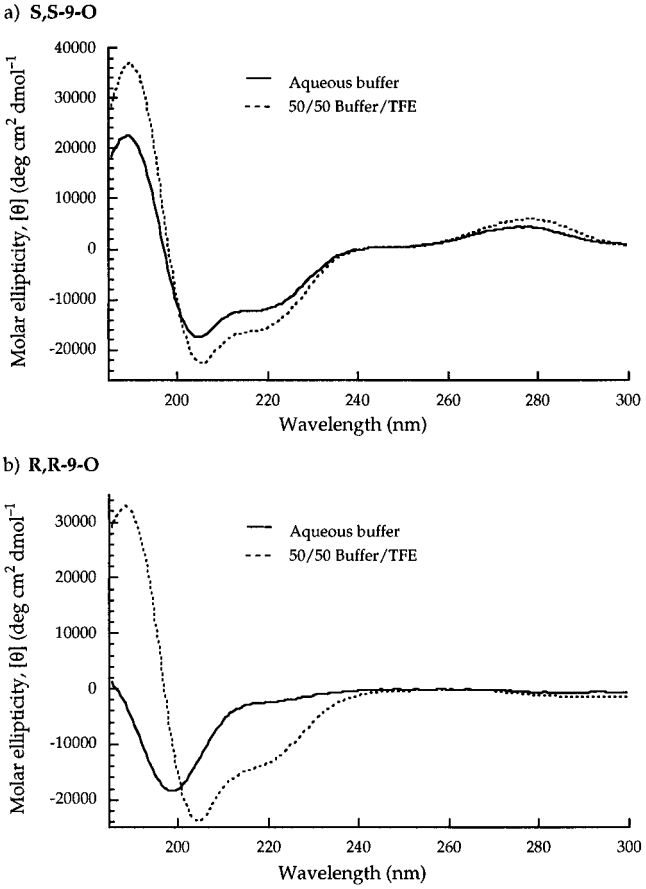

Figure 5. Comparison of CD spectra of (a) **S,S-9-O** and (b) **R,R-9-O** in aqueous buffer and 50:50 buffer/2,2,2-trifluoroethanol (0 °C).

character in 50% TFE/buffer, as reflected in their molar ellipticities at 222 nm, indicating that the peptides behave normally and adopt the α-helical conformation under these conditions. TFE titration indicates that the helicity observed in 50% TFE/buffer is the maximum that these conjugates can attain; the molar ellipticity determined under these conditions thus provides an alternative benchmark for estimating helical character under different conditions. In fact, the ellipticity exhibited by **S,S-9-O** in aqueous buffer at 0 °C is 77% of the limiting value observed in 50% TFE, which is considerably higher than the value calculated from the traditional formula.[37,38]

The divergent behavior of **S,S-9-O** and the *R,R*-stereoisomer supports a clear role for the template in inducing helical behavior in aqueous solution. However, the protonation state of the template carboxylate is also a critical feature: comparison of the CD spectra of **S,S-9-O** at different pH values shows that the templating effect is lost when the carboxylate is protonated (Figure 6). Spectra taken as a function of pH show two isodichroic points, consistent with a simple two-state equilibrium between helix and random coil. Protonation of the glutamate side chain at lower pH and loss of any salt-bridging interaction with lysine may also contribute to the decrease in helical character as well.

As reported before for other templated helical conjugates,[11,17] there is no dramatic temperature dependence of the molar ellipticity (Figure 7). In particular, there is no inflection representative of a cooperative melting process, and significant helicity persists up to 70 °C.

(32) Toniolo, C.; Polese, A.; Formaggio, F.; Crisma, M.; Kamphuis, J. *J. Am. Chem. Soc.* **1996**, *118*, 2744−2745.

(33) The ellipticity measured at 222 nm for the helical conjugates arises from the peptide only, since the template ester does not absorb significantly in the region 200−270 nm (see Figure S4 in the Supporting Information). The negative ellipticity at 275 nm observed in the peptide conjugate of one of the diastereomeric templates, tentatively assigned as **R,S-9-O** (Figure 4b), arises from subtraction of a positive peak in the spectrum of **R,S-10-O**.

(34) Storrs, R. W.; Truckses, D.; Wemmer, D. E. *Biopolymers* **1992**, *32*, 1695−1702.

(35) Jasanoff, A.; Fersht, A. R. *Biochemistry* **1994**, *33*, 2129−2135.

(36) Cammers-Goodwin, A.; Allen, T. J.; Oslick, S. L.; McClure, K. F.; Lee, J. H.; Kemp, D. S. *J. Am. Chem. Soc.* **1996**, *118*, 3082−3090.

(37) Chen, Y. H.; Yang, J. T.; Chau, K. H. *Biochemistry* **1974**, *13*, 3350−3359.

(38) Engel, M.; Williams, R. W.; Erickson, B. W. *Biochemistry* **1991**, *30*, 3161−3169.

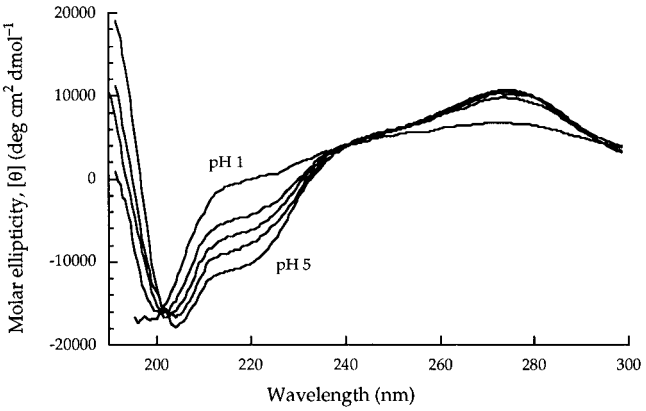

Figure 6. Effect of pH on CD spectrum of **S,S-9-O** in aqueous solution (0 °C). Shown are spectra obtained at pH 5, 4, 3, 2, and 1; spectra at pH 8, 7, 8, and 9 were superimposable with that at pH 5.

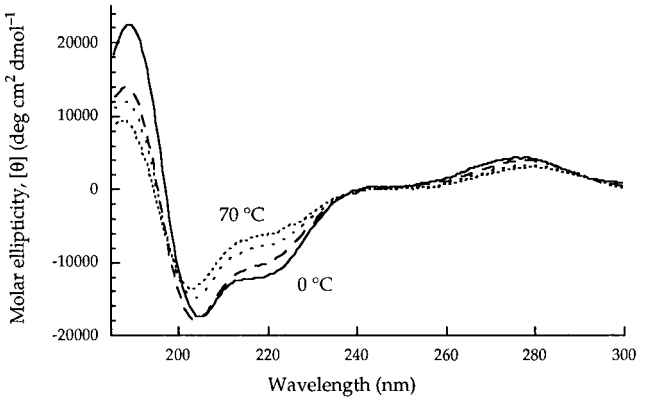

Figure 7. Effect of temperature on CD spectrum of **S,S-9-O** in aqueous solution at 0, 30, 50, and 70 °C.

The success of the ester-linked template and failure of the amide-linked design lend credence to the rationale behind this alteration, namely, prevention of the hydrogen-bonding pattern illustrated in Figure 3. We envisaged an alternative strategy for preventing this interaction sterically, in the form of the neutral dimethylamide **9-N-a**. This template would be able to

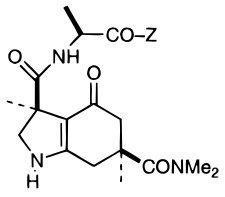

S,S-8-N-a: Z = OMe
S,S-9-N-a: Z = EALAKA–NH$_2$

enter into the desired hydrogen-bonding interaction, with the dimethylamino group bisecting the substituents at C-6; however, the undesired, transannular interaction would force one of the amide methyls to eclipse the C-6 methyl group (Figure 8). Although it is the most straightforward route to this analog, direct formation of the dimethylamide at C-6, after selective cleavage of the *tert*-butyl ester in **6**, proved difficult to effect in good yield. The *S,S*- and *R,R*-diastereomers of the L-alanine amide **8-N-a** were therefore synthesized from *N,N*-dimethyl-3,5-dimethoxybenzamide by a route analogous to that shown in Scheme 2.

The dimethylamide derivative was not effective as a helix template. The CD spectra indicate that both the *S,S*- and *R,R*-diastereomers of **9-N-a** are predominantly random coil in aqueous solution, although they are otherwise normal in their response to TFE (data not shown). This result, as well as the pH dependence for conjugate **S,S-9-O** (Figure 6), underscores the importance of a negatively charged carboxylate at the C-6 position. This charge presumably helps to complement the macrodipole of the helix, as generally observed for negatively charged amino acids at the N-terminus.[39]

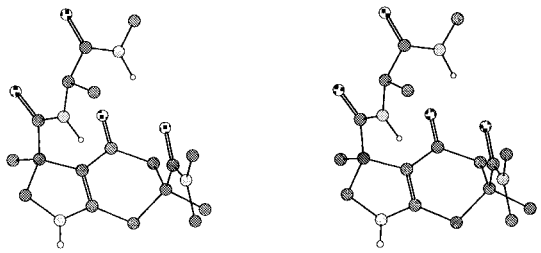

Figure 8. Proposed templating conformation of dimethylamide conjugate **S,S-9-N-a**.

The absolute strength of the hydrogen bonds formed by the various templates is not, to a first approximation, the critical factor in determining the position of equilibrium between the helical and random coil forms of the peptide conjugates. As the NH-to-carbonyl bond strength decreases from **S,S-9-N** to **S,S-9-O** in the templated conformation, so does the strength of the hydrogen bond(s) between that oxygen and water in the solvated form (eq 1). For this reason, we interpret the ineffectiveness of the amide **S,S-9-N** as arising from the hydrogen-bonding pattern of Figure 3 and that of amide **S,S-9-N-a** from the lack of charge complementarity.

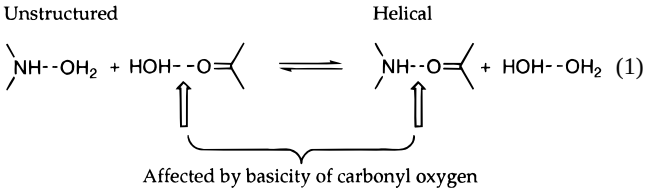

Characterization by NMR

Although CD gives quantitative information on conformational equilibria, it is time-averaged and global in nature. NMR, in contrast, provides structural information at the single-residue level as well as insight into the dynamical behavior of the oligopeptide chain. The nuclear Overhauser effect (NOE) provides the most important parameter for elucidating the conformation of a peptide since it has a strong, $1/r^6$ dependence on the internuclear distance. The observation of a direct NOE between a pair of protons is evidence for a significant population of conformers in which the protons are close, typically within 3.5 Å for flexible peptides in solution.[40] The distance between the $C_\alpha H$ of residue i and the NH of the following residue (i+1), represented by $d_{\alpha N}$(i, i+1), is a short 2.2 Å in the extended conformation of a peptide, and this contact can be detected even if the population of this conformer is relatively small. In contrast, the threshold population for observation of the medium-range $d_{\alpha N}$(i, i+3) NOEs characteristic of helical conformations is relatively high, since the distance is 3.4 Å.[41] Such medium range NOEs are typically weak and high signal-to-noise NOESY or ROESY spectra are required for their detection.[42]

Certain inter-residue NOE patterns are characteristic of specific secondary structures, since these structural elements have regular geometries and defined hydrogen−hydrogen

(39) Doig, A. J.; Baldwin, R. L. *Protein Sci.* **1995**, *4*, 1325−1336.
(40) Wüthrich, K. *NMR of Proteins and Nucleic Acids*; John Wiley & Sons: New York, 1986.
(41) Waltho, J. P.; Feher, V. A.; Lerner, R. A.; Wright, P. E. *FEBS Lett.* **1989**, *250*, 400−404.

distances. For example, the geometry of the α-helix is characterized by short distances between residues i and i+3 and i and i+4; in the more tightly wound 3_{10}-helix, short distances occur between residues i and i+2 and i and i+3; and in tight turns, close contacts also occur between residues i and i+2. *β*-Sheet structures, in contrast, consist of extended polypeptide segments in which medium-range distances are absent.[44]

Short $d_{\alpha N}$(i, i+1) distances and thus strong $d_{\alpha N}$(i, i+1) NOE connectivities indicate backbone dihedral angles in the *β* (extended chain) region of (*ϕ*, *ψ*) space; these $d_{\alpha N}$(i, i+1) NOEs normally dominate NOESY spectra of unfolded ("random coil") peptides in aqueous solution. In contrast, helical residues are connected throughout by short d_{NN}(i, i+1) distances; hence, the observation of d_{NN}(i, i+1) NOE connectivities is evidence that the conformational ensemble of the peptide includes α-helical or turnlike structures. The simultaneous observation of extended regions of $d_{\alpha N}$(i, i+1) and d_{NN}(i, i+1) connectivities for an oligopeptide indicates conformational averaging between the α- and *β*-regions of (*ϕ*, *ψ*) space. Adjacent (i to i+1) $d_{\alpha N}$ and d_{NN} NOE connectivities provide information only on individual backbone dihedral angles and do not identify extended regions of helical or *β*-strand structure.[43] However, a sequence of consecutive NOEs is more robust evidence for a particular secondary structure; for example, sequences of 3−5 successive distance constraints $d_{NN} < 3.6$ Å enable helical segments to be identified with high reliability,[44] especially when some medium-range NOEs can also be identified in this segment.

Assignment of Resonances. The one dimensional (1D) ^{1}H NMR spectra of the N-terminally capped peptide **S,S-9-O** and the acetylated comparison peptide (Ac-AEALAKA-NH_2, **13**) were recorded at 4 °C in 50 mM phosphate, 100 mM KCl buffer in 10% D_2O/H_2O at pH 4.2, to permit the observation of exchangeable protons. A jump-and-return selective excitation sequence[45] was used to avoid saturation transfer from water to the exchangeable protons. The ^{1}H NMR spectrum of **S,S-9-O** is characterized by narrow line widths, good signal-to-noise ratio, and a large chemical shift dispersion within the envelope of the amide protons (Figure 9a), which is indicative of a significant population of stable, compact conformations. On the other hand, the chemical shift dispersion within the envelope of the CαH protons is poor, as typically seen in small helical proteins rather than in regions of *β*-structure or in random coil peptides.[46] The acetylated analog **13** shows a much narrower chemical shift range for the amide protons, as expected for a more flexible, unstructured peptide.

We assigned the 1D ^{1}H NMR spectra in the sequence specific manner devised by Wüthrich,[40] tracing a continuous pathway along the peptide backbone using alternating COSY connectivities within a residue (NH−αH) and sequential NOESY connectivities, $d_{\alpha N}$(i, i+1) and d_{NN}(i, i+1), between adjacent residues, as illustrated in Figure 10.

The side chain spin systems for leucine, lysine, and glutamate were assigned from their scalar coupling networks and the relayed connectivities observed in TOCSY spectra. The NH−αH intraresidue connectivities were identified in spectra acquired in 90% H_2O/10% D_2O by direct connectivity or by TOCSY relay to resonances farther out the side chain. In this manner, the parent spin systems of all the amide protons were identified (Figure 9b).[47]

The sequential assignment of resonances for **S,S-9-O** was obtained from NOESY and TOCSY spectra recorded under the standard conditions (pH 4.2, 4 °C in 90% H_2O/10% D_2O). In spite of the low chemical shift dispersion in the CαH proton envelope of the reference 1D spectrum, intraresidue NH−αH connectivities in the TOCSY spectrum gave rise to a series of nonoverlapping cross peaks (see Figure 9b). Although the signal-to-noise ratio of the NOESY spectrum used for the sequential assignment was lower than that of the TOCSY spectrum, a complete set of sequential d_{NN}(i, i+1) connectivities could nonetheless be obtained (Figure 11). However, the jump-and-return read sequence in the former pulse program gave rise to less-efficient suppression of the residual water signal, and as a result, the NH−αH connectivities could not be observed in the f_2 dimension. For conjugate **S,S-9-O**, d_{NN}(i, i+1) connectivities were used for the assignment because poor digital resolution in the f_1 dimension (256 t_1 increments), as well as the low chemical shift dispersion for the α-hydrogens, made it difficult to identify $d_{\alpha N}$(i, i+1) connectivities. In contrast, the inter-residue NOEs observed for the acetylated peptide **13** were $d_{\alpha N}$(i, i+1) rather than d_{NN}(i,i+1) connectivities (data not shown), as expected for an unstructured peptide. All chemical shifts assigned for the peptides and the bicyclic cap of **S,S-9-O** and **13** are listed in Table 2.

The observation of a series of d_{NN}(i, i+1) connectivities spanning the entire six-residue sequence in the NOESY spectra of **S,S-9-O** (Figure 11) suggests that helical conformers dominate the population for this conjugate; the distribution of $d_{\beta N}$(i, i+1) NOEs is also consistent with this interpretation.[44] However, the relative intensities of $d_{\alpha N}$(i, i+1) and d_{NN}(i, i+1) NOEs indicate that extended chain conformers are also part of the ensemble. As unambiguous evidence for the helical conformer, we sought medium-range NOEs, e.g., $d_{\alpha N}$(i, i+3), $d_{\alpha\beta}$(i, i+3), $d_{\alpha\beta}$(i, i+4) etc. The $d_{\alpha N}$ NOE region of the NOESY spectrum of **S,S-9-O** is depicted in Figure 12. The severe resonance overlap of CH_β protons in the region $\delta = 1.44-1.46$ ppm and CH_α protons in the region $\delta = 4.15-4.22$ ppm made it difficult to distinguish medium-range and side chain−side chain NOEs from intraresidue connectivities. As a result, only one of four possible $d_{\alpha N}$(i, i+3) NOEs was observed (Ala-7/Leu-4 NH−αH).[48]

Amide Proton Temperature Coefficients. The magnitude of the temperature dependence of an amide proton chemical shift is generally accepted as a measure of the degree to which it is engaged in an intramolecular hydrogen bond;[49,50] smaller

(42) While NOEs are sensitive indicators of folded structures within a conformational ensemble, quantitative estimation of a population size from relative NOE build up rates is complicated by conformational averaging and the $1/r^6$ dependence of the NOE.[43] Consequently, we have used the 2D spectra qualitatively, simply to identify conformations whose populations in aqueous solution exceed the threshold value for observation of diagnostic NOEs.

(43) Dyson, H. J.; Wright, P. E. *Ann. Rev. Biophys. Chem.* **1991**, *20*, 519−538.

(44) Wüthrich, K.; Billeter, M.; Braun, W. *J. Mol. Biol.* **1984**, *180*, 715−740.

(45) Plateau, P.; Gueron, M. *J. Am. Chem. Soc.* **1982**, *104*, 7310−7311.

(46) Wishart, D. S.; Sykes, B. D.; Richards, F. M. *J. Mol. Biol.* **1991**, *222*, 311−334.

(47) In routine 1D ^{1}H NMR spectra that were recorded, several low-intensity signals were observed within the amide envelope (see Figure 9a); TOCSY spectra confirmed the peptidic nature of these resonances, as spin systems corresponding to alanine and glutamate were identified. Since neither the broadening of these resonances over the range of 277−323 K nor the chemical exchange of the cross peaks was observed between the two sets of amide proton resonances in the NOESY spectrum, we concluded that a small amount of uncapped peptide as a contaminant, rather than a minor conformer of **S,S-9-O**, was responsible. In any event, the resonances from the impurity did not interfere with those of the conjugate **S,S-9-O** or complicate their interpretation.

(48) The molecular mass (907 Da) of the capped peptide is such that the molecular correlation time may fall near the zero NOE region ($\omega_o\tau_c = 1$). At 4 °C, tumbling is slowed to the extent that the peptide falls into the negative NOE regime, as evidenced by cross peaks of the same sign as the diagonal in the 2D NOESY spectra recorded at this temperature. 2D ROESY spectra were acquired under spin-locked conditions to overcome this limitation; however, additional medium-range NOEs were not apparent in spectra recorded with mixing times (T_m) of 250 and 400 ms.

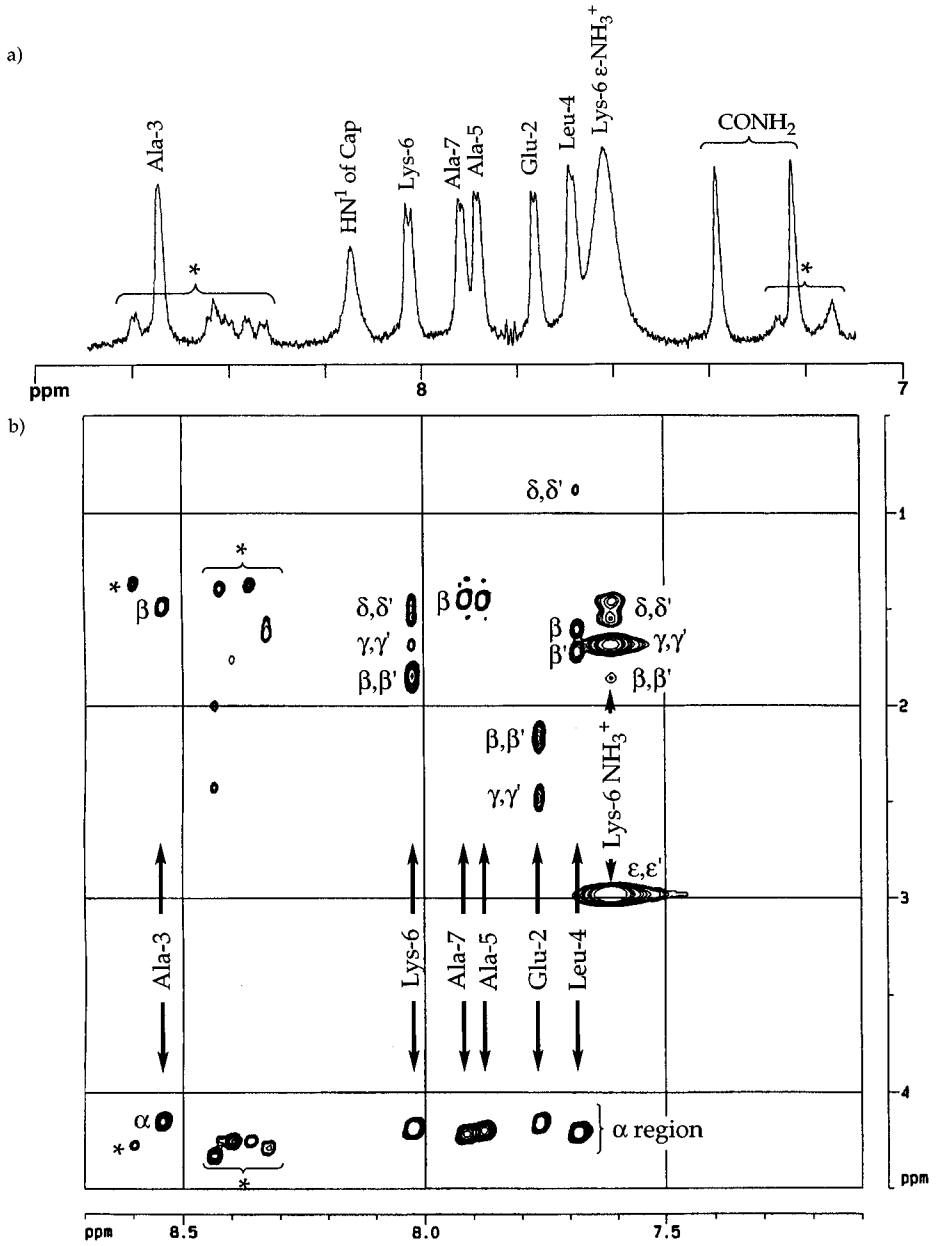

Figure 9. (a) Amide NH region of 1D spectrum of conjugate **S,S-9-O** (3.8 mM, 90% H_2O/10% D2O, pH 4.2, 4 °C) (the asterisk denotes cross peaks from uncapped peptide); (b) TOCSY spectrum showing NH to side chain cross peaks.

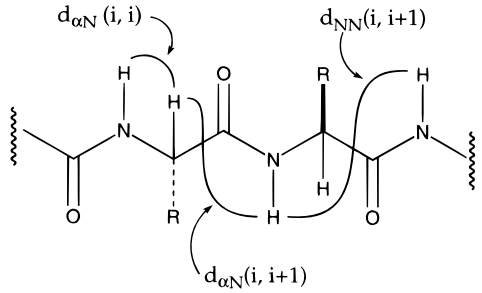

Figure 10. Intra- and inter-residue connectivities employed in the sequential assignment of resonances.

values ($\Delta\delta$ < 3−4 ppb/K) are observed if the NH is involved in an intrachain hydrogen bond as part of a defined secondary structure than if it is exposed to solvent water ($\Delta\delta \approx 8$ ppb/K). The temperature coefficients for the amide hydrogens in the peptide conjugate **S,S-9-O** and the comparison analog **13** were determined from spectra acquired in 90% H_2O/10% D_2O over the temperature range of 4−62 °C (Figure 13 and Table 3); solvent suppression was achieved with a jump-and-return read sequence to ensure that the NH resonances were not attenuated by saturation transfer from water.

The values calculated for the temperature coefficients represent averages over the conformational ensemble of the peptide and conjugate; as a result, intermediate values are expected if both helical and extended conformations are represented significantly. The low temperature coefficients observed for all of the residues of **S,S-9-O** except Ala-3 are consistent with a dominant conformation in which the amide protons are part of hydrogen-bonding networks of a defined secondary structure. The higher temperature dependence of the Ala-3 NH chemical shift is anomalous in this series, with a value that corresponds to a solvated amide. It is unclear whether the high value arises from dislocation of this amide from the anticipated helical structure or from the vinylogous amide carbonyl as an atypical hydrogen-bonding partner.

(49) Kessler, H. *Angew. Chem., Int. Ed. Engl.* **1982**, *21*, 512−523.
(50) Dyson, H. J.; Cross, K. J.; Houghten, R. A.; Wilson, I. A.; Lerner, R. A. *Nature* **1985**, *318*, 480.

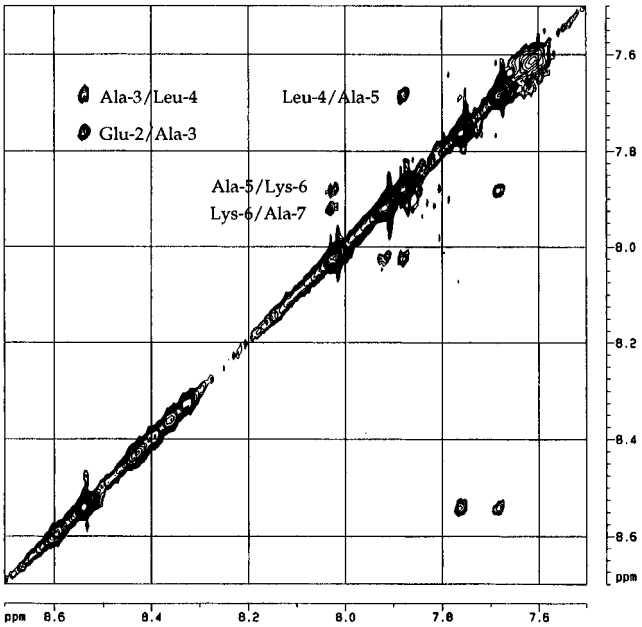

Figure 11. Jump-and-return NOESY spectrum of **S,S-9-O** illustrating d_{NN}(i, i+1) sequential NOEs (T_m = 800 ms, pH 4.2, 4 °C).

$^3J_{HN\alpha}$ Coupling Constants. The magnitude of the $^3J_{HN\alpha}$ coupling constant observed in a polypeptide chain is dependent on the ϕ-angle and therefore on the local conformation of the polypeptide backbone (Figure 14). While $^3J_{HN\alpha}$ values for β-sheet conformations fall in the range from 8 to 10 Hz ($-150° < \phi < -90°$), helices are characterized by $^3J_{HN\alpha}$ values between 4 and 5 Hz ($-70° < \phi < -30°$).[51] A series of three or more coupling constants below 6 Hz has been taken as diagnostic of helical structure.[43]

The $^3J_{HN\alpha}$ values for conjugate **S,S-9-O** could be measured directly from the 1D spectrum over the temperature range of 4−50 °C because of the excellent chemical shift resolution within the amide envelope. The coupling constants determined at 4 and 25 °C are presented with the corresponding ϕ torsion angles in Table 4.

For all residues, the coupling constants measured at 4 °C average 4.1 Hz, which is close to the value of 3.9 Hz predicted for the ideal helix geometry. Larger values are observed at 25 °C, consistent with an increase in the proportion of extended and random coil conformers relative to helix as thermal unfolding occurs. Nevertheless, the coupling constants remain less than 7 Hz, even up to 42 °C, suggesting that a significant population of helical conformers persists. The absence of a defined unfolding or melting temperature was observed in the CD spectrum of this conjugate and has been described previously for other templated peptides.[11,17]

Dynamical Behavior of Peptide Conjugate S,S-9-O. The ability of the cap to prevent N-terminal fraying of the α-helix in **S,S-9-O** can be assessed by analyzing the dynamical behavior of the peptide backbone, which is revealed by the relaxation properties of the amide bond vector (^{1}H−^{15}N). Of particular use in interpreting protein backbone dynamics are the NOE and T_1 and T_2 relaxation rates,[52,53] which are dependent on the spectral density function at five characteristic frequencies ($J(0)$, $J(\omega_N)$, $J(\omega_H)$, $J(\omega_H - \omega_N)$, and $J(\omega_H + \omega_N)$). Sampling the spectral density function fully at these five frequencies requires a set of six relaxation measurements.[54,55] However, a simplified, model-free formalism introduced by Lipari et al.[56,57] allows analysis of backbone dynamics from only three relaxation measurements (T_1, T_2, and NOE), which are represented by eqs 2−4.[58]

$$\frac{1}{T_1} = d^2[J(\omega_H - \omega_N) + 3J(\omega_N) + 6J(\omega_H + \omega_N)] + c^2J(\omega_N) \quad (2)$$

$$\frac{1}{T_2} = 0.5d^2[4J(0) + J(\omega_H - \omega_N) + 3J(\omega_N) + 6J(\omega_H + \omega_N)] + \frac{c^2[3J(\omega_N) + 4J(0)]}{6} \quad (3)$$

$$\mathrm{NOE} = 1 + T_1\frac{\gamma_H}{\gamma_N}d^2[6J(\omega_H + \omega_N) - J(\omega_H - \omega_N)] \quad (4)$$

where

$$d^2 = \frac{\gamma_H^2\gamma_N^2(h/2\pi)^2}{r_{HN}^3} \text{ and } c^2 = \frac{2}{15}\omega_N^2(\sigma_{||} - \sigma_\perp)^2$$

$\hbar$ is Planck's constant, γ_H and γ_N are the ^{1}H and ^{15}N gyromagnetic ratios, ω_H and ω_N are the ^{1}H and ^{15}N Larmor frequencies, r_{HN} is the ^{1}H−^{15}N internuclear distance (1.02 Å[53]), and $\sigma_{||}$ and $\sigma_\perp$ are the parallel and perpendicular components of the assumed axially symmetric ^{15}N shift tensor ($\sigma_{||} - \sigma_\perp$) = −160 ppm.[59]

In the model-free formalism, these three relaxation parameters provide a measure of dynamic behavior that is specific to each residue. The approach is based on a simplified spectral density function (eq 5), with the assumption that the molecule undergoes isotropic tumbling.

$$J(\omega) = \frac{2}{5}\left[\frac{S^2\tau_m}{1 + (\omega\tau_m)^2} + \frac{(1 - S^2)\tau}{1 + (\omega\tau)^2}\right], \text{ where } \frac{1}{\tau} = \frac{1}{\tau_m} + \frac{1}{\tau_e} \quad (5)$$

The effective correlation time, τ_e, represents the reorientation of the N−H bond vector with respect to the overall tumbling time of the molecule itself, τ_m. S^2, the generalized order parameter, is a measure of the extent to which internal motion is coupled to that of the molecule as a whole; S^2 can range from 0, for independent isotropic motion, to 1, for completely restricted motion. In proteins, these values generally extend from ca. 0.5 for disordered loop regions to ca. 0.85 for well-defined secondary structures.[53] These parameters are obtained from a fit of the spectral density function (eq 5) with the relationships describing the experimentally determined relaxation rates (eqs 2−4).[60,61]

The data acquired at 4 °C on a sample of **S,S-9-O** uniformly ^{15}N-labeled from Glu-2 to Ala-7 indicate limited backbone motion for residues 3−5, with increasing motion for Lys-6 and

(51) Pardi, A.; Billeter, M.; Wüthrich, K. *J. Mol. Biol.* **1984**, *180*, 741.
(52) Kay, L. E.; Torchia, D. A.; Bax, A. *Biochemistry* **1989**, *28*, 8972−8979.
(53) Clore, G. M.; Driscoll, P. C.; Wingfield, P. T.; Gronenborn, A. M. *Biochemistry* **1990**, *29*, 7387−7401.
(54) Peng, J. W.; Wagner, G. *J. Magn. Reson.* **1992**, *98*, 308−332.
(55) Peng, J. W.; Wagner, G. *Biochemistry* **1992**, *31*, 8571−8586.
(56) Lipari, G.; Szabo, A. *J. Am. Chem. Soc.* **1982**, *104*, 4559−4570.
(57) Lipari, G.; Szabo, A. *J. Am. Chem. Soc.* **1982**, *104*, 4546−4559.
(58) Abragham, A. *The Principles of Nuclear Magnetism*; Claredon Press: Oxford, England, 1961.
(59) Hiyama, Y.; Niu, C.; Silverton, J. V.; Bavaso, A.; Torchia, D. A. *J. Am. Chem. Soc.* **1988**, *110*, 2378−2383.
(60) Palmer, A. G. I.; Rance, M.; Wright, P. E. *J. Am. Chem. Soc.* **1991**, *113*, 4371−4380.
(61) Orekhov, V. Y.; Nolde, D. E.; Golovanov, A. P.; Korzhnev, D. M.; Arseniev, A. S. In *Shemyakin and Ovchinnikov*; Institute of Bio-Organic Chemistry, Russian Academy of Sciences: Moscow, 1995.

Table 2. Assignment of Template Peptide Conjugate **S,S-9-O** (3.5 mM) and, in Parentheses, Acetylated Peptide **13** (5.8 mM)[a]

residue	NH	αH[b]	β,β′H	γ,γ′H	δ,δ′H	ϵ,ϵ′H
Lac-1/(Ala-1)	n/a (8.48)	4.810 (4.167)	1.46 (1.36)			
Glu-2	7.76 (8.69)	4.160 (4.195)	2.16 (1.96, 2.03)	2.46, 2.50 (2.30)		
Ala-3	8.54 (8.31)	4.150 (4.222)	1.48 (1.37)			
Leu-4	7.68 (8.12)	4.207 (4.252)	1.71 (1.65)	1.60 (1.58)	0.87 (0.86, 0.91)	
Ala-5	7.88 (8.22)	4.195 (4.219)	1.45 (1.39)			
Lys-6	8.02 (8.25)	4.185 (4.233)	1.84 (1.77, 1.85)	1.68 (1.67)	1.46, 1.54 (1.45)	2.98 (2.99)
Ala-7	7.91 (8.26)	4.215 (4.227)	1.44 (1.41)			

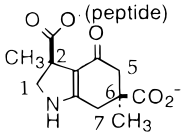

C-1,1′	C-5,5′	C-7,7′	C-2-Me	C-6-Me
2.43, 2.64	3.59, 4.15	2.61, 3.00	1.33	1.44

[a] In 90% H_2O/10% D_2O, pH 4.2, at 4 °C; chemical shifts referenced to internal dioxane (δ = 3.74 ppm). [b] Recorded to three decimal places because of low dispersion in αH chemical shifts.

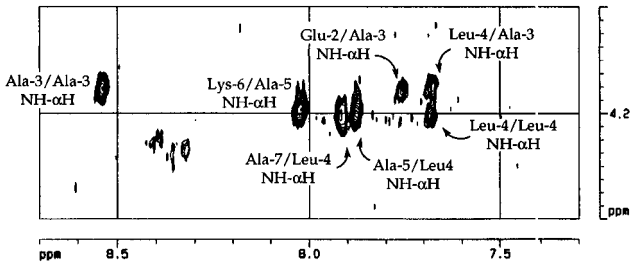

Figure 12. Jump-and-return NOESY spectrum of **S,S-9-O** illustrating $d_{\alpha N}$ connectivities (T_m = 800 ms, pH 4.2, 4 °C).

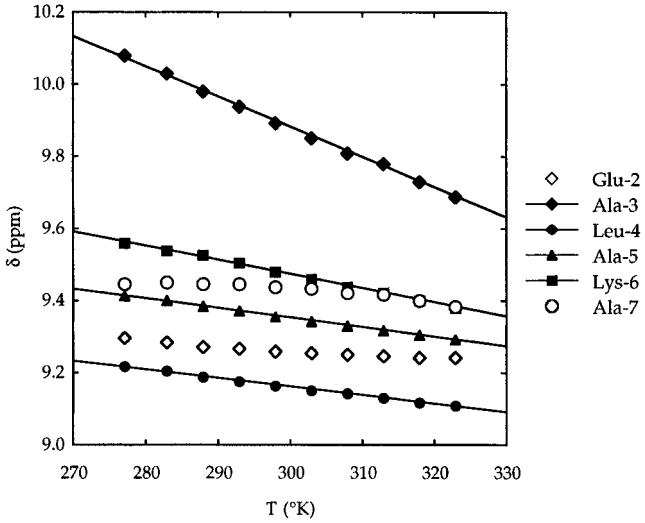

Figure 13. Temperature dependence of the chemical shifts of the amide protons of **S,S-9-O** (3.8 mM, pH 4.2).

Table 3. Temperature Dependence of Amide Proton Chemical Shifts (Δδ, ppb/K) for Conjugate **S,S-9-O** and Acetylated Peptide **13**[a]

	Ala-1	Glu-2	Ala-3	Leu-4	Ala-5	Lys-6	Ala-7
S,S-9-O		>−1.2[b]	−8.5	−2.4	−2.7	−3.9	>−1.4[b]
13	−8.0	−6.5	−6.2	−6.2	−6.3	−7.0	−6.2

[a] Coefficients were determined over the temperature range of 4−52 °C. A negative sign indicates a shift to lower frequency with increasing temperature. [b] Nonlinear relationship observed for δ vs $1/T$ for this residue (see Figure 13).

Ala-7 and, interestingly, Glu-2 (Figure 15). The S^2 values suggest the presence of a well-defined secondary structure in the center of the peptide, with the motion at Ala-7 approaching that of a dynamic loop. This behavior is consistent with S^2 profiles typically observed for α-helices, which show lower order parameters for the ends of the helix where fraying occurs.[62]

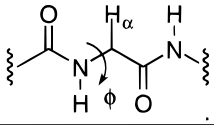

	ϕ (°)	$^3J_{NH,\alpha H}$ (Hz)
Antiparallel β-sheet	−139°	9.0
Parallel β-sheet	−119	9.7
α-Helix	−57	3.9
3_{10}-Helix	−49	3.0

Figure 14. Relationship between secondary structure and ϕ torsion angle.[40,51]

Table 4. $^3J_{\alpha N}$ Coupling Constants (Hertz) and Corresponding Average ϕ Torsional Angle, Determined from the Amide Proton Resonances for Conjugate **S,S-9-O**

	Glu-2	Ala-3	Leu-4	Ala-5	Lys-6	Ala-7
4 °C	4.1	*a*	4.1	3.6	5.2	3.7
ϕ^b	−59		−59	−55	−68	−56
25 °C	5.1	3.2	5.8	5.0	6.2	5.3
ϕ^b	−67	−51	−73	−67	−76	−69

[a] Coupling constant not resolved. [b] The corresponding ϕ-angles are determined from the equation: $^3J_{\alpha N} = 6.4\cos^2\theta - 1.4\cos\theta + 1.9$ ($\theta = \phi - 60$).[50]

The low S^2 value for Glu-2 may reflect its proximity to the template−lactate ester linkage; the ester is not as strongly hydrogen bonded as the peptide amides and may undergo a crankshaft-like rotation that increases the mobility of the neighboring NH bond vector.

Conclusions

The bicyclic template **S,S-9-O**, when linked to a peptide through an ester linkage, is unusually effective in inducing the α-helical conformation, with some 50−75% helicity observed in the conjugate with lactyl-Glu-Ala-Leu-Ala-Lys-Ala-amide, as determined by circular dichroism spectroscopy. The templating ability is directly related to the stereochemistry of the template, and it is characterized by a relative insensitivity to temperature and a strong dependence on the ionization state of the terminal carboxyl group. It is apparent that the template must complement the N-terminus of the α-helix both sterically as well as electronically to be effective. By the global, time-averaged view afforded by CD spectroscopy, the template induces helical character in a short peptide to an unprecedented extent.

The NMR investigations provide insight into the effects of the helix template on the local conformation and dynamical

(62) Redfield, C.; Boyd, J.; Smith, L. J.; Smith, R. A. G.; Dobson, C. M. *Biochemistry* **1992**, *31*, 10431−10437.

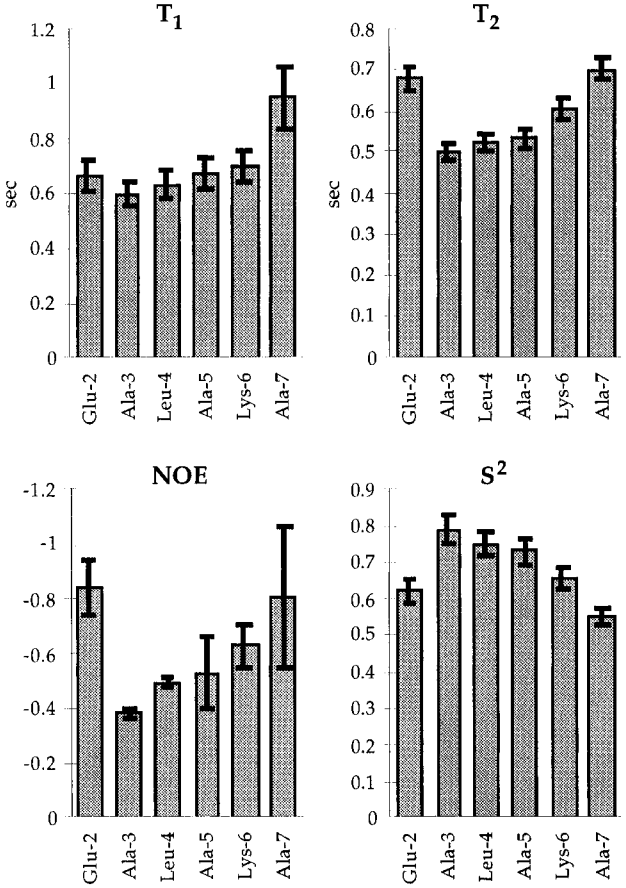

Figure 15. Relaxation rates and characterization of dynamical behavior of ^{15}N-labeled **S,S-9-O** (pH 4.2, 4 °C).

behavior of conjugate **S,S-9-O**. The data are consistent with a conformational ensemble for **S,S-9-O** in which helical conformers are dominant, and they indicate that the template works by reducing the fraying at the N-terminus of the peptide, as intended. The NMR results are thus consistent with the chiroptical studies, which together suggest that the template will be useful in probing structural effects on helical behavior and the role of helical peptide conformations in ligand−receptor and protein−protein interactions.

Experimental Section

***tert*-Butyl 4-(1-Methoxycarbonyl-2-nitroethyl)-1-methyl-3,5-dioxocyclohexanecarboxylate (3).** *tert*-Butyl 3,5-dimethoxybenzoate[63] (11.51 g, 44 mmol) and *tert*-butyl alcohol (4.59 mL, 48 mmol) were dissolved in 50 mL of THF. Ammonia (200 mL) was distilled from sodium into the flask at −78 °C, and potassium (4.5 g, 15 mmol) was added in small pieces until the solution remained blue. Methyl iodide (14.9 mL, 240 mmol) was filtered through alumina, diluted with 50 mL of THF, and added to the solution, which turned from blue to brown and then to a light yellow. The solution was stirred at −78 °C for 2 h, the ammonia was allowed to evaporate under a stream of N_2, and the reaction mixture was concentrated under reduced pressure. The residue was dissolved in water and extracted several times with ether, and the organic layer was dried ($MgSO_4$) and concentrated to 10.3 g (84%) of *tert*-butyl 3,5-dimethoxy-1-methylcyclohexa-2,5-dienecarboxylate, which was carried on directly to the hydrolysis step.

A solution of the alkylation product (5.09 g, 20 mmol) and mercuric nitrate (2.26 g, 6.6 mmol) in 140 mL of CH_3CN and 30 mL of water was heated to reflux under N_2 for 12 h. The reaction mixture was concentrated, dissolved in aqueous NaCl solution, and extracted with three portions of EtOAc. The organic layer was dried ($MgSO_4$) and concentrated, and the crude product was chromatographed (95:5 CH_2Cl_2/methanol) to give 3.88 g (86%) of *tert*-butyl 1-methyl-3,5-dioxocyclohexanecarboxylate (**2**) as a light brown solid: IR ($CHCl_3$) 2970, 1720, 1590 cm^{-1}; ^{1}H NMR δ 3.35 (dt, 1, J = 18.0, 1.7), 3.28 (d, 1, J = 18.0), 2.83 (dd, 2, J = 1.7, 15.6), 2.51 (dd, 2, J = 1.0, 15.6), 1.37 (s, 9), 1.31 (s, 3); ^{13}C NMR δ 201.7, 172.9, 83.6, 56.1, 50.0, 41.8, 27.6, 24.2; MS (EI) *m/z* 226 (3.38), 211 (6.21), 202 (8.33), 186 (12.19), 170 (33.26), 153 (34.24), 125 (58.52), 57 (100), 56 (99.38).

A solution of methyl β-nitroacrylate[26,64] (2.03 g, 15.5 mmol) as a solution in methanol (62 mL) was added *via* cannula to a solution of the diketone **2** (3.50 g, 15.5 mmol) and triethylamine (1.56 g, 2.15 mL, 15.5 mmol) in methanol (85 mL) at 0 °C. After 2 h, the cooling bath was removed and the solution was stirred at room temperature for 24 h. The mixture was concentrated under reduced pressure, and the residue was dissolved in CH_2Cl_2 (100 mL) and washed successively with 0.5 N HCl (25 mL) and brine (25 mL). The organic phase was dried ($MgSO_4$) and concentrated *in vacuo* to give the Michael adduct **3** (5.46 g, 15.2 mmol, 99% yield): IR (film) 2980, 1730, 1550, 1380 cm^{-1}; ^{1}H NMR δ 4.99 (dd, 1, J = 8.3, 13.8), 4.71 (dd, 1, J = 6.1, 8.3), 4.29 (dd, 1, J = 6.0, 13.8), 3.66 (s, 3), 2.95 (d, 1, J = 17.0), 2.94 (d, 1, J = 17.0), 2.44 (d, 1, J = 17.0), 2.42 (d, 1, J = 17.0), 1.40 (s, 9), 1.31 (s, 3); ^{13}C NMR δ 173.9, 171.7, 109.6, 81.9, 73.4, 53.4, 52.4, 43.6, 42.1, 42.0, 37.1, 27.6, 27.5, 24.5. Anal. Calcd for $C_{16}H_{23}NO_8$: C, 53.78; H, 6.49; N, 3.92. Found: C, 53.50; H, 6.60; N, 3.59.

Methyl 6-*tert*-Butoxycarbonyl-6-methyl-2,3,4,5,6,7-hexahydroindol-4-one-3-carboxylate (4). A slurry of the Michael adduct **3** (2.67 g, 7.48 mmol) and Raney Nickel (2.24 g, washed with water until the filtrate was neutral to pH paper, followed by washing with methanol) in methanol (25 mL) was placed under a 50 psi atmosphere of H_2 and shaken for 65 h. The mixture was filtered through Celite, the filtrate was evaporated, and the residue was chromatographed (95:5, CH_2Cl_2/methanol) to give the vinylogous amide **4** (1.94 g, 6.28 mmol, 84% yield) as a mixture of diastereomers: IR (film) 3200, 2985, 1730, 1575, 1160 cm^{-1}; ^{1}H NMR δ 3.71−3.83 (m, 3), 3.59 (s, 3), 2.80 (d, 1, J = 16.7), 2.55 (d, 1, J = 16.1), 2.27 (d, 1, J = 16.7), 2.19 (d, 1, J = 16.2), 1.29 (s, 9), 1.20 (s, 3); ^{13}C NMR δ 187.6, 174.5, 174.2, 169.3, 106.4, 80.8, 51.9, 50.8, 45.6, 45.3, 42.9, 33.0, 27.6, 24.0; MS (EI) *m/z* 309 (24.84), 250 (46.99), 236 (33.26), 208 (56.36), 194 (78.11), 148 (74.71), 120 (60.55), 106 (42.79), 80 (85.98), 57 (97.90), 41 (100); HRMS (EI) calcd for $C_{16}H_{23}NO_5$ 309.1577; found 309.1587.

Methyl 1,6-Di-*tert*-butoxycarbonyl-6-methyl-2,3,4,5,6,7-hexahydroindol-4-one-3-carboxylate (5). To the bicyclic ester **4** (1.27 g, 4.13 mmol) in 200 mL of CH_2Cl_2 was added 2-((*tert*-butoxycarbonyloxy)imino)-2-phenylacetonitrile ("Boc-ON", 1.22 g, 4.96 mmol) and KH (199 mg, 4.96 mmol). The mixture was stirred under N_2 at room temperature for 22 h and then washed with 1:1 satd. K_2CO_3 until no more UV activity was observed in the aqueous layer. The organic layer was washed with brine, dried ($MgSO_4$), and concentrated, and the residue was chromatographed (silica, 2:1 hexanes/EtOAc) to give **5** as two diastereomers.

Higher R_f diastereomer: 944 mg (56%); ^{1}H NMR δ 4.00 (m, 2), 3.80 (m, 1), 3.71 (s, 3), 2.76 (d, 1, J = 4.2), 2.71 (s, 1), 2.33 (d, 1, J = 16.2), 1.49 (s, 9), 1.37 (s, 9), 1.32 (s, 3); ^{13}C NMR δ 191.8, 174.5, 173.4, 150.7, 116.6, 83.0, 81.3, 60.3, 52.5, 46.1, 45.6, 41.6, 34.9, 28.1, 27.8, 24.7; MS (EI) *m/z* 409 (2), 336 (2), 309 (5), 280 (7), 250 (15), 208 (31), 194 (45), 57 (100). Anal. Calcd for $C_{21}H_{31}NO_7$: C, 61.60; H, 7.63; N, 3.42. Found: C, 61.45; H, 7.71; N, 3.35.

Lower R_f diastereomer: 601 mg, 36%; ^{1}H NMR δ 4.05 (s, 1), 4.03 (d, 1, J = 1.6), 3.87 (m, 1), 3.68 (s, 3), 2.82 (dd, 1, J = 1.2, 16.4), 2.62 (dd, 1, J = 2.2, 18.6), 2.23 (d, 1, J = 16.4), 1.50 (s, 9), 1.39 (s, 9), 1.31 (s, 3).

Methyl (3*RS*,6*RS*)- and (3*RS*,6*SR*)-1,6-Di-*tert*-butoxycarbonyl-3,6-dimethyl-2,3,4,5,6,7-hexahydroindol-4-one-3-carboxylate (*cis*-6 and *trans*-6). To a solution of the Boc-protected diester (mixture of isomers, 3.49 g, 8.55 mmol), methyl iodide (6.07 g, 2.66 mL, 42.8 mmol), and hexamethylphosphoric triamide (HMPA) (3.83 g, 3.72 mL, 21.4 mmol) in THF (67 mL) at −78 °C was added lithium hexamethyldisilazide (LiHMDS) (12.0 mL, 12.0 mmol, 1.0 M in THF) *via* addition funnel over a period of 15 min. After 30 min, acetic acid (721 mg, 687 μL, 12.0 mmol) was added, and the mixture was warmed to room temperature and concentrated under reduced pressure. The

(63) Crowther, G. P.; Kaiser, E. M.; Woodruff, R. A.; Hauser, C. R. *Org. Synth.* **1971**, *51*, 96−100.

(64) Shechter, H.; Conrad, F. *J. Am. Chem. Soc.* **1953**, *75*, 5610−5613.

residue was dissolved in EtOAc (100 mL), washed with brine (25 mL), dried ($MgSO_4$), and concentrated, and the residue was chromatographed (2:1, hexanes/EtOAc) to give the monomethylated product (3.03 g, 7.18 mmol, 84% yield) as an oil. The diastereomers were separated by MPLC on a Lobar Lichroprep Si 60 column, size C, using a 3:1 hexane/EtOAc mixture as solvent, monitoring at 254 nm; the maximum amount injected under these conditions was 1.4 g. For *cis*-**6** (higher R_f diastereomer): ^{1}H NMR δ 4.05 (d, 1, J = 11.6), 3.63 (s, 3), 3.59 (d, 1, J = 11.5), 2.74 (d, 1, J = 16.2), 2.66 (d, 1, J = 18.5), 2.23 (d, 1, J = 16.2), 1.49 (s, 9), 1.44 (s, 3), 1.39 (s, 9), 1.28 (s, 3); ^{13}C NMR δ 191.5, 174.4, 174.2, 150.9, 82.8, 81.2, 60.7, 52.4, 48.1, 46.5, 45.3, 34.7, 28.1, 27.7, 24.9, 22.3. For *trans*-**6** (lower R_f diastereomer): ^{1}H NMR δ 4.03 (d, 1, J = 11.7), 3.68 (s, 3), 3.60 (d, 1, J = 11.7), 2.72 (d, 1, J = 16.1), 2.63 (d, 1, J = 18.4), 2.26 (d, 1, J = 16.2), 1.49 (s, 9), 1.41 (s, 3), 1.37 (s, 9), 1.30 (s, 3); ^{13}C NMR δ 191.5, 174.8, 174.4, 150.9, 82.9, 81.3, 60.8, 52.6, 47.9, 46.4, 45.7, 36.6, 35.0, 28.1, 27.9, 27.8, 25.0, 22.5; MS (FAB) *m/z* 424 $(MH)^+$. Anal. Calcd for $C_{22}H_{33}NO_7$: C, 62.39; H, 7.85; N, 3.31. Found: C, 62.17; H, 7.88; N, 3.34.

(3*RS*,6*RS*)-6-*tert*-Butoxycarbonyl-3,6-dimethyl-2,3,4,5,6,7-hexahydroindol-4-one-3-carboxylic Acid (*cis*-7). A solution of the ester *cis*-**6** (725 mg, 1.72 mmol) and 2 N NaOH (1.89 mL, 3.78 mmol) in 50% aqueous methanol (28 mL) was heated at 80 °C for 24 h. After cooling the reaction to room temperature, the solution was evaporated, and the residue was dissolved in water (15 mL). The aqueous solution was carefully acidified to pH = 2 by the addition of 1 N HCl and extracted with CH_2Cl_2 (3 × 15 mL), and the combined organic fractions were dried ($MgSO_4$) and evaporated to give the carboxylic acid *cis*-**7** (454 mg, 1.47 mmol, 85% yield). ^{1}H NMR indicated >95% purity as well as complete removal of the Boc group. For *cis*-**7**: ^{1}H NMR (400 MHz) δ 6.78 (s, 1), 4.31 (d, 1, J = 11.8), 3.45 (d, 1, J = 11.8), 2.92 (d, 1, J = 16.8), 2.76 (d, 1, J = 16.5), 2.39 (d, 1, J = 16.5), 2.33 (d, 1, J = 16.8), 1.53 (s, 3), 1.36 (s, 9), 1.29 (s, 3); ^{13}C NMR δ 190.2, 177.0, 174.0, 170.5, 108.6, 82.0, 57.3, 51.5, 45.9, 44.6, 33.8, 27.7, 24.9, 24.4; MS (FAB) *m/z* 310 $(MH)^+$; HRMS (FAB) calcd for $C_{16}H_{24}NO_5$ 310.1655, Found 310.1656.

Compound *trans*-**7** was prepared from *trans*-**6** in a similar fashion: ^{1}H NMR (400 MHz) δ 7.20 (s, 1), 4.28 (d, 1, J = 12.0), 3.46 (d, 1, J = 12.0), 2.95 (d, 1, J = 16.9), 2.84 (d, 1, J = 16.9), 2.32 (d, 1, J = 16.9), 2.26 (d, 1, J = 16.6), 1.45 (s, 3), 1.39 (s, 9), 1.31 (s, 3); ^{13}C NMR δ 189.1, 177.5, 174.0, 171.6, 108.8, 81.7, 57.5, 51.4, 46.0, 44.4, 33.8, 27.8, 25.3, 24.9.

(3*R*,6*R*)- and (3*S*,6*S*)-*O*-(1,6-Di-*tert*-butoxycarbonyl-3,6-dimethyl-3-oxo-2,3,4,5,6,7-hexahydroindol-4-one)-L-lactate Methyl Ester (R,R-12-O and S,S-12-O). A slurry of KH (115 mg, 2.87 mmol, washed with hexane) and Boc-ON (292 mg, 1.19 mmol) in THF (11 mL) was stirred at 0 °C, and a solution of ***cis*-7** (334 mg, 1.08 mmol) in THF (11 mL) was added *via* cannula. On completion of the addition, the cooling bath was removed and the reaction mixture was stirred at room temperature for 24 h. A solution of 0.5 M HCl (25 mL) was added, the resulting mixture was extracted with CH_2Cl_2 (3 × 50 mL), and the combined extracts were dried ($MgSO_4$) and evaporated to give a mixture of the BOC-protected compound ***cis*-11** and oxime side product (621 mg).

The crude Boc-protected product was dissolved in THF (7 mL) with triethylamine (240 mg, 0.331 mL, 2.38 mmol) and 2,4,6-trichlorobenzoyl chloride (580 mg, 0.372 mL, 2.38 mmol). After 2 h, the cloudy mixture was filtered through a plug of glass wool, the amine hydrochloride salt was washed with THF, and the filtrate was concentrated *in vacuo*. The residue was dissolved in toluene (10 mL) and methyl L-lactate (337 mg, 0.309 mL, 3.24 mmol) and DMAP (791 mg, 6.48 mmol) were added. The flask was equipped with a reflux condenser and immersed in a preheated (110 °C) oil bath. After 3.5 h, the solution was cooled, diluted with ether (40 mL), washed sequentially with 0.5 N HCl (20 mL), water (20 mL), saturated $NaHCO_3$ (20 mL), and water (20 mL), dried (MgSO4), and evaporated. The residue was first purified by flash chromatography (2:1, hexane/EtOAc) to give the template lactate ester **12-O** as a mixture of diastereomers (400 mg, 806 mmol, 70% yield for four steps). The diastereomers were separated by MPLC on a Lobar Lichroprep Si 60 column, size C, employing 2.5:1 hexane/EtOAc as mobile phase, monitoring at 254 nm. The less-polar compound was identified as **R,R-12-O** by chemical correlation to **R,R-8-N** (as described in the Supporting Information).

For **S,S-12-O**: ^{1}H NMR (500 MHz, $CDCl_3$) δ 5.09 (q, 1, J = 7.1), 4.20 (d, 1, J = 11.7), 3.71 (s, 3), 3.65 (d, 1, J = 11.7), 3.54 (d, 1, J = 18.4), 2.82−2.74 (m, 2), 2.26 (d, 1, J = 16.2), 1.54 (s, 3), 1.53−1.50 (m, 12), 1.40 (s, 9), 1.30 (s, 3).

For **R,R-12-O**: ^{1}H NMR (500 MHz, $CDCl_3$) δ 5.12 (q, 1, J = 7.1), 4.20 (d, 1, J = 11.6), 3.71 (s, 3), 3.69−3.66 (m, 1), 3.54 (d, 1, J = 18.5), 2.80 (d, 1, J = 18.7), 2.75 (d, 1, J = 16.4), 2.26 (d, 1, J = 16.4), 1.52 (s, 9), 1.45 (s, 3), 1.42−1.40 (m, 12), 1.31 (s, 3).

HRMS (FAB) characterization of the *R,S*-diastereomer, prepared from ***trans*-6** by the same procedure: calcd for $C_{25}H_{38}NO_9$ 496.2547, found 496.2533.

General Procedure for the Preparation of Templated Peptides 9-O by Solid Phase Peptide Synthesis. To a solution of the methyl ester **12-O** (0.0323−0.114 mmol) in 25% aqueous methanol (1−2 mL) was added 1 N LiOH (1.2 equiv). The resulting mixture was stirred at room temperature for 1−2 h and then concentrated under reduced pressure. The residue was dissolved in water (15 mL) and carefully acidified to pH = 2 with 1 N HCl. The resulting solution was extracted with CH_2Cl_2 (3 × 15 mL), and the combined organic fractions were dried ($MgSO_4$) and concentrated *in vacuo* to give the monocarboxylic acid (61−88% yield).

The Fmoc-EALAKA-Rink resin[65] (gift of Reyna Simon and Simon Ng of Chiron Corporation; 1.25 equiv) was allowed to swell in DMF (1.5 mL) for 1 h. DMF was removed by filtration, and the resin was washed with additional DMF (1.5 mL). The resin was treated with 20% piperidine in DMF (2 × 1.5 mL, 3 and 10 min) to remove the Fmoc protecting group, filtered, and washed with additional DMF (10 × 1.5 mL). A solution of the carboxylic acid prepared above, ethyl 2-(dimethylamino)ethyl carbodiimide (EDC, 1 equiv), and 1-hydroxybenzotriazole (HOBT, 1 equiv) in DMF (1.5 mL) was added to the resin and the slurry was stirred for 1 h. The resin was filtered, washed with DMF (2 × 1.5 mL) followed by CH_2Cl_2 (2 × 1.5 mL), and stored under vacuum overnight.

The resin was treated with cleavage reagent R (90% trifluoroacetic acid (TFA), 5% thioanisole, 3% ethanedithiol, 2% anisole; 5 mL) under N_2 for 2.5 h.[66] The mixture was filtered through glass wool into cold ether, and the solution was stored at 0 °C overnight. The fluffy white precipitate that formed was collected on a fine frit, washed with cold ether, and stored under vacuum overnight. The peptide conjugate was purified by reverse phase HPLC using a two-solvent system (solvent A 90% H_20, 10% CH_3CN, 0.1% TFA; solvent B 10% H_20, 90% CH_3CN, 0.1% TFA) with programmed elution (0 min, 100% A; 30 min, 50% A, 50% B; 40 min, 100% B; 50 min, 100% B; 60 min, 100% A) on a Vydac C18 prep column, monitored at 304 nm.

(3*S*,6*S*)-(3,6-Dimethyl-6-(hydroxycarbonyl)-3-oxo-2,3,4,5,6,7-hexahydroindol-4-one)-L-lactyl-Glu-Ala-Leu-Ala-Lys-Ala-NH_2 (S,S-9-O): LRMS (FAB) 908.4 (MH^+); HRMS (FAB) calcd for $C_{41}H_{66}N_9O_{14}$ 907.4729, found 907.4725.

(3*R*,6*R*)-(3,6-Dimethyl-6-(hydroxycarbonyl)-3-oxo-2,3,4,5,6,7-hexahydroindol-4-one)-L-lactate-Glu-Ala-Leu-Ala-Lys-Ala-NH_2 (R,R-9-O): LRMS (FAB) 908.5 (MH^+).

Circular Dichroism (CD) Measurements. All stock solutions were prepared with doubly distilled water. Spectra of pure buffer were obtained for each temperature and subtracted from the spectra for each peptide. The concentrations of stock solutions of the **9-N**, **10-N**, **9-O**, and **10-O** diastereomers were determined by measuring the UV absorbance in water at 307 nm (ϵ_{307} = 14 400). The ϵ value was determined by careful dilution of a precisely weighed sample of **S,R-9-N** in CH_3CN and measurement of the absorption at 304 nm (red shift due to decreased solvent polarity). The concentration of the control peptide Ac-AEALAKA-NH_2 was determined from amino acid analysis. The observed ellipticities were corrected by subtraction of the measured ellipticities of reference samples of the corresponding cap itself in buffer (**10-N** or **10-O**), either measured at the same concentration as the peptide conjugate or scaled to the same concentration prior to subtraction.

(A) Diastereomers of 9-N and 10-N. The standard buffer solution was 0.1 M KCl and 50 mM potassium phosphate, with the pH adjusted to 5.2 by the addition of 1.0 M KOH. Spectra were obtained on a

(65) Rink, H.; Sieber, P. In *Peptides 1988*; Jung, G., Bayer, E., Eds.; Walter de Gruyter & Company: Berlin, 1989; pp 139−141.

(66) Hudson, D. In *Peptides 1988*; Jung, G., Bayer, E., Eds.; Walter de Gruyter & Company: Berlin, 1989; pp 211−213.

Jasco J-600 spectropolarimeter at 15 μM concentration in a 1.0 cm Hellma cylindrical cell. A Neslab Instruments circulating ethylene glycol/water cooling unit connected to the jacketed cell was used for temperature regulation. With this arrangement, high absorbance prevented accurate measurements below 200 nm. The temperature was allowed to stabilize for at least 15 min before a spectrum was recorded. The spectra were obtained from 200 to 260 nm at a scan speed of 20 nm/min and 4 scans per run. The sensitivity was ±50 mdeg, the time constant was 2.0 s, and the band width was 1.0 nm with a 0.2 nm step resolution.

(B) Diastereomers of 9-O and 10-O. The standard buffer was 1.05 mM KH_2PO_4 buffer at pH 5.0; spectra were recorded in 0.2 cm, strain-free cells on an Aviv 62 DS spectropolarimeter with thermojacketed cell holder. Spectra were obtained over the range of 185−300 nm; 5 scans were typically recorded with a band width of 1.5 nm, 0.5 nm step size, and 1 s time constant. Temperature melts were recorded over the range of 0.5−70 °C at 222 nm with a 30 s averaging time, 2−5 °C step size, and 3−5 min equilibration time.

Synthesis of ^{15}N-Labeled Conjugate. $^{15}N^{\alpha}$-Labeled amino acids were obtained from Cambridge Isotopes. $^{15}N^{\alpha}$-Glutamic acid and $^{15}N^{\alpha}$-lysine were converted to the N^{α}-Fmoc-derivatives with *tert*-butyl and Boc side chain protection, respectively, as described in the Supporting Information; $^{15}N^{\alpha}$-leucine was converted to the Fmoc derivative by the standard procedure, and $^{15}N^{\alpha}$-Fmoc-alanine was available commercially. The side chain-protected, $^{15}N^{\alpha}$-containing hexapeptide EALAKA was prepared on Rink resin and coupled to the cap-L-lactic acid as described above. After purification by reverse phase chromatography (with the desired product eluting at ∼24% CH_3CN/H_2O), the $^{15}N^{\alpha}$-labeled conjugate **S,S-9-O** was obtained as a white powder and characterized by mass spectrometry (FAB *m/z* 914 (MH^+)) and ^{1}H NMR spectroscopy.

Sample Preparation. Solutions for the observation of exchangeable protons were prepared by dissolving the conjugate in 500 μL of buffer containing 50 mM potassium phosphate and 0.1 M KCl, lyophilizing, and dissolving the residue in 450 μL of H_2O and 50 μL of D_2O at a concentration of 3.5 mM in conjugate. The sample pH recorded within the NMR tube was 4.2; unless otherwise stated, all spectra were recorded at this pH.

NMR Experimental Details. ^{1}H NMR spectra were recorded on a Bruker AM 500 spectrometer equipped with an Aspect 3000 computer, and data were processed using the Bruker UXNMR software package. 1D spectra in 90% H_2O/10% D_2O were recorded using a jump-and-return selective excitation sequence, $(\pi/2)-D2-(\pi/2)-$acquire.[45] The carrier frequency was set on the water signal with a delay time, D2, of 140 μs to ensure that there would be effective excitation over the envelope of amide protons. 2D experiments were recorded at a probe temperature of 4 °C in the phase-sensitive mode using the time-proportional phase incrementation method of Marion and Wüthrich[67] for quadrature detection in f_1. The same spectral widths were used as in the 1D experiments. Between 8 and 32 transients of 2048 data points each were typically recorded in the f_2 dimension and 256−512 t_1 increments were recorded and zero-filled to 1024 data points. In cases where high digital resolution was required in f_1, up to 1024 t_1 increments were collected and zero-filled to 2048 data points. Prior to Fourier transformation, spectra were zero-filled once in the f_1 dimension and subjected to a phase-shifted sine bell weighting function in both dimensions.

Phase-sensitive NOESY spectra were recorded using a jump-and-return[45] read pulse with the overall sequence $(\pi/2)-t_1-(\pi/2)-\tau_m-(\pi/2)-D2-(\pi/2)-$acquire (D2 = 140 μs). Mixing times (T_m) of 200, 400, and 800 ms were used with a 20 ms *z*-filter to remove zero quantum artifacts and appropriate phase cycling to select *z*-magnetization. The initial value of t_1 was set to 3 μs.

TOCSY[68] spectra were recorded with a 50 ms MLEV-17 spin-locking pulse.[69] Phase coherent solvent suppression was achieved using a DANTE[70,71] sequence (pulse width 25 μs and inter-pulse delay of 250 μs) applied for 1.7 s before the start of each transient.

For NMR spectra recorded over a range of temperatures, the temperature of the probe was calibrated using solutions of analytical grade methanol or ethylene glycol by the method of Van Geet.[72] Chemical shifts were referenced to internal dioxane (δ = 3.74 ppm).

NMR measurements of ^{15}N-labeled material were recorded at 600.14 MHz (^{1}H) and 60.819 MHz (^{15}N) on a Bruker AMX-600 at 4 and 37 °C. Spectral widths of 1094.74 and 6024.10 Hz were used in F_1 and F_2, respectively, with a total of 2K complex data points collected in F_2. Phase sensitivity was achieved using TPPI.[67] Water-suppression was achieved using a combination of trim pulses[73] and low-power presaturation. Measurements of the ^{15}N T_1 and T_2 values were carried out using the pulse programs described by Barbato[74] with relaxation delays of 26, 54, 96, 250, 503, 797, and 1499 ms for T_1 (each time point was recorded twice) and 8, 39, 79, 181, 605, 909, and 1500 ms for T_2 (each time point was recorded one or two times). A recycle delay of 2.5 s was used and 29 complex t_1 increments of 32 scans each were acquired. The relaxation times T_1 and T_2 were obtained from exponential fits of the peak height data. NOE experiments were carried out according to Skelton et al.[75] in which two data sets were collected, one with the NOE and one without. A recycle delay of 5 s was used, and 29 complex t_1 increments of 64 scans were acquired. The NOE effect was calculated as the ratio of peak heights in the two spectra collected with and without NOE.

^{15}N NMR Relaxation Calculations. The ^{15}N relaxation data for conjugate **S,S-9-O** was analyzed using the formalism of Lipari and Szabo for isotropic tumbling.[56,57] Model-free parameters were obtained by substituting the spectral density expression (eq 5) into those describing the dependence of the relaxation rate constants T_1 and T_2, and the heteronuclear NOE on the spectral density values (eqs 2−4); the experimentally measured values were used to optimize the fit with the software programs MODELFREE3.1 and DNMR.[60,61]

Acknowledgment. This work was supported by a grant from the National Institutes of Health (no. GM-30759 to P.A.B.); A.M.S. and W.N.H. received support from NIH Training Grants nos. GM08295 and GM-08352, respectively. P.A.B. has been on appointment as a Miller Research Professor in the Miller Institute for Basic Research in Science. D.E.W., C.W.L., and H.S.C are supported through the Director, Office of Energy Research, Office of Biological & Environmental Research, General Life Science Division of the U.S. Department of Energy under contract no. DE-AC03-76F00098. An instrumentation grant to D.E.W. was provided by the NSF (BBS 87-20134). We thank Prof. Susan Marqusee (Molecular and Cell Biology, UC Berkeley) for assistance with the CD measurements, Dr. Reyna Simon and Simon Ng (Chiron Corporation) for solid phase synthesis of the hexapeptide precursor, Georges Lauri for molecular dynamics simulations of the template peptides, and Kathy Lee for bringing the word "aglet" to our attention.

Supporting Information Available: Experimental procedures and characterization of the compounds not described above; representative CD spectra of the diastereomers of **9-N** and **9-N-a**; temperature and concentration dependence of CD spectrum of **S,S-9-O**; preparation of α-Fmoc-α-^{15}*N*-glutamic acid γ-*tert*-butyl ester and α-Fmoc-ε-Boc-α-^{15}*N*-lysine; and full TOCSY spectrum of **S,S-9-O** (17 pages). See any current masthead page for ordering and Internet access instructions.

JA964231A

(67) Marion, D.; Wüthrich, K. *Biochem. Biophys. Res. Commun.* **1983**, *113*, 967−974.
(68) Braunschweiler, L.; Ernst, R. R. *J. Magn. Reson.* **1983**, *53*, 521−528.
(69) Bax, A.; Davis, D. G. *J. Magn. Reson.* **1985**, *65*, 355−360.
(70) Morris, G. A.; Freeman, R. *J. Magn. Reson.* **1978**, *29*, 433−462.
(71) Zuiderweg, E. R. P.; Hallenga, K.; Olejniczak, E. T. *J. Magn. Reson.* **1986**, *70*, 336−343.
(72) Van Geet, A. L. *Anal. Chem.* **1968**, *40*, 2227−2229.
(73) Messerle, B. A.; Wider, G.; Otting, G.; Weber, C.; Wüthrich, K. *J. Magn. Res.* **1989**, *85*, 608−613.
(74) Barbato, G.; Ikura, M.; Kay, L. E.; Pastor, R. W.; Bax, A. *Biochemistry* **1992**, *31*, 5269−5278.
(75) Skelton, N. J.; Palmer, A. G. I.; Akke, M.; Kördel, J.; Rance, M.; Chazin, W. J. *J. Magn. Res., Ser. B* **1993**, *102*, 253−264.
(76) The more conservative n = 7 was chosen, although the contribution from the first Ala residue may be compensated by the controls **7-N** or **7-O**.